

Article

Study on the Adsorption Characteristics of Calcareous Sand for Pb(II), Cu(II) and Cd(II) in Aqueous Solution

Gang Li ¹, Deqiang Yan ¹, Jinli Zhang ^{2,*}  and Jia Liu ³ ¹ Shaanxi Key Laboratory of Safety and Durability of Concrete Structures, Xijing University, Xi'an 710123, China² State Key Laboratory of Coastal and Offshore Engineering, Dalian University of Technology, Dalian 116024, China³ School of Geological Engineering and Geomatics, Chang'an University, Xi'an 710054, China

* Correspondence: jlzhang@dlut.edu.cn

Abstract: The adsorption characteristics of calcareous sand for heavy metals Pb(II), Cu(II) and Cd(II) have been studied by batch testing in this study. The influence of the solid–liquid ratio, initial pH₀ value, ionic strength, reaction time, temperature and initial concentration on adsorption has been investigated. Test results indicate that the initial pH and the solid–liquid ratio have a significant influence on the removal efficiency. At $T = 30\text{ }^{\circ}\text{C}$, $r = 1.0\text{ g/L}$, and $C_0 = 1000\text{ mg/L}$ and for 12 h of reaction, the removal efficiencies of Pb(II), Cu(II) and Cd(II) are 97.6%, 88.15% and 65.72%, respectively. The adsorption quantity is more than 80% of the maximum adsorption quantity within 60 min, and the equilibrium adsorption can be reached within 120 min. The pseudo-second-order kinetic model is suitable to simulate the dynamic adsorption process of calcareous sand, and the isothermal process is found to obey the Langmuir model. Calcareous sand has a very high adsorption capacity for Pb(II), Cu(II) and Cd(II), with a maximum adsorption quantity Q_m reached 1052.95 mg/g, 1329.84 mg/g and 1050.56 mg/g, respectively. Thermodynamic test results indicate that the adsorption process is spontaneously exothermic and that low temperature is favorable to the adsorption reaction.

Keywords: calcareous sand; heavy metal ions; adsorption; pH; temperature



Citation: Li, G.; Yan, D.; Zhang, J.; Liu, J. Study on the Adsorption Characteristics of Calcareous Sand for Pb(II), Cu(II) and Cd(II) in Aqueous Solution. *Sustainability* **2023**, *15*, 5372. <https://doi.org/10.3390/su15065372>

Academic Editors: Yawei Shi, Jun Wang and Zonglin Pan

Received: 18 February 2023

Revised: 13 March 2023

Accepted: 16 March 2023

Published: 17 March 2023



Copyright: © 2023 by the authors. Licensee MDPI, Basel, Switzerland. This article is an open access article distributed under the terms and conditions of the Creative Commons Attribution (CC BY) license (<https://creativecommons.org/licenses/by/4.0/>).

1. Introduction

After entering soil or water, heavy metals accumulate in the migration process due to their non-degradable properties; they are enriched in animals and plants and subsequently enter the human body through the food chain, posing severe threats to human health [1]. Lead is a widely used industrial material used in printing and dyeing, chemical engineering processes and batteries. By far the main treatment methods for industrial wastewater are chemical precipitation, ion exchange, electrochemistry and adsorption [2]. Relative to other methods, the adsorption method has the advantages of simple utilization conditions and low cost and therefore has received extensive attention. The key challenge of the method is to find cheap, high-efficiency adsorbents [3].

Studies have shown that clay, bentonite, kaolin, bone black, carbon nanotube-hydroxyapatite and other adsorbents have favorable lead-removal qualities [4–7]; for example, the adsorption of lead by loess can reach 270.26 mg/g [8]. Saha et al. [9] studied the adsorption characteristics of clay for copper; at pH = 5.5, the removal rate was 90–99%. Abdel-Halim et al. [10] examined the adsorption characteristics of bone powder, activated carbon, carbon, rose plant powder, clay and other adsorbents for lead. They reported that at pH = 4, the removal rates of bone powder and activated carbon were 100% and 90%, respectively. Singh et al. [11] investigated the lead adsorption characteristics of phosphate-containing clay. Their results showed that the removal rate of lead increased with increasing phosphate-containing clay and increasing pH and decreased with increasing ionic strength. The main adsorption mechanism was the exchange of lead ions and calcium ions, producing stable pyromorphite. Vieira et al. [12] studied the influencing parameters and kinetics of nickel

adsorption by bentonite. Priyantha and Bandaranayaka [13] analyzed the adsorption ability of clay bricks for Cr(VI) under different heating temperatures; the adsorption mechanism was internal diffusion between pores and particles. Djukić et al. [14] showed that the cation exchange ability of Serbian clay was greatly improved after ball milling; the removal rate of lead and chromium was higher than 98%. Du and Hayashi [15] studied the adsorption characteristics and influencing factors of clay in Kyushu, Japan for chromium and lead. The results of Mouni et al. [16] showed that Algerian clay had a higher affinity for lead than zinc. Waseem et al. [17] revealed that the adsorption of Cd(II) onto silica synthesized by the sol–gel method was endothermic and spontaneous, and the adsorption capacity increased with increasing concentration and temperature. Putz et al. [18] indicated that the adsorption capacities of ordered mesoporous silica to Cu(II) and Pb(II) reached 9.7 mg/g and 18.8 mg/g at pH 5, respectively. Habte et al. [19] reported that the adsorption capacity of aragonite synthesized by eggshell was higher for Pb(II) than Cd(II), and high adsorption capacity occurred at an initial pH of 6. Vu et al. [20] concluded that the adsorption capacities toward levofloxacin and diclofenac reached 75.75 mg/g and 59.52 mg/g, indicating that protein-functionalized nanosilica was a potential adsorbent for removing pharmaceutical residues. Truong et al. [21] reported that the optimum adsorption of Cu-doped ZnO nanomaterial toward Cu(II) were achieved under the conditions of pH 7, adsorption time 120 min and adsorption efficiency at 1.0 g/L.

Calcareous soils are potential adsorbents for wastewater treatment, which has been confirmed by scholars. Selmy [22] investigated the adsorption characteristics of Pb in soils treated with inorganic ligands, and found that the maximum adsorption capacities of Pb onto clay soil changed from 42.2 to 47.1 mmol/kg. Based on a miscible displacement column experiment, Elbana and Selim [23] reported that the adsorption efficiency of Pb reached 99.5% with calcareous soil. Lv et al. [24] indicated that calcareous sand is a potential adsorbent for graphene oxide (GO), and the adsorption process significantly depends on pH value. Salzman et al. [25] concluded that fluoride is adsorbed by calcareous and siliceous sand during drier summer months, while desorption occurs during rainy winter months. Ranjbar and Jalali [26] found that the average adsorption quantity of NH_4^+ by calcareous soil reached 35.23%. Baghenejad et al. [27] observed that the selectivity adsorption sequence on calcareous soils followed $\text{Pb} > \text{Cu} > \text{Zn} > \text{Cd}$. Ghiri et al. [28] investigated the adsorption and desorption characteristics of Zn on calcareous soils, and found that Zn adsorption followed clay > silt > sand. Moharami and Jalali [29] concluded that silt, clay, sand, and electrical conductivity (EC) were the major factors affecting Fe adsorption in calcareous soils. Based on principal component analysis method, Mashal et al. [30] investigated the adsorption and desorption behaviors of P on calcareous soils, and found that the sand and clay content are the major factors for modeling P adsorption. Ouachtak et al. [31,32] investigated the adsorption characteristics of goethite-modified sand, and concluded that the adsorbed capacity toward gallic acid decreases with presence of inorganic anions, and decrease with ionic strength increasing. In addition, the maximum adsorbed capacity toward 3,4-dihydroxybenzoic acid reached 35.66 mg/kg under the condition of 60 mg/L initial concentration, 1 mL/min flow rate, and 5 pH value.

Calcareous sand is widely distributed in the South China Sea. Its main components are bone fragments of coral, algae, shellfish and other marine life. Its mineral composition is mainly aragonite, dolomite, and calcite, with large amounts of calcium carbonate and magnesium carbonate (above 96%) [33,34]. Calcareous sand has the characteristics of loose porosity, fragility, easy compression, and high permeability. Current studies indicated that calcareous sand was a potential adsorbent onto heavy metals ions, whereas few studies focus on the adsorption characteristics of calcareous sand towards Pb(II), Cu(II) and Cd(II). In this paper, calcareous sand was used as an adsorbent to study the effect of the solid–liquid ratio, initial pH_0 value, temperature and reaction time on the adsorption characteristics for Pb(II), Cu(II) and Cd(II); to explore the kinetic characteristics and isothermal characteristics; and to analyze the adsorption mechanism.

2. Materials and Methods

2.1. Experimental Materials

The tests used South China Sea calcareous sand. After rinsing the calcareous sand, it was pulverized by a high-speed pulverizer and sieved with a 160-mesh sieve. The calcareous sand was then dried at 75 °C in a drying oven (DHG-9011A, Shanghai Jinghong Laboratory Instrument Co., Ltd., Shanghai, China) for 4 h. After cooling to room temperature, it was stored in a dry container with CaO. Figure 1 shows the SEM image of calcareous sand. It can be observed that the sand particles have the characteristics of multiple pores (including internal pores), irregular shape, and high fragility.

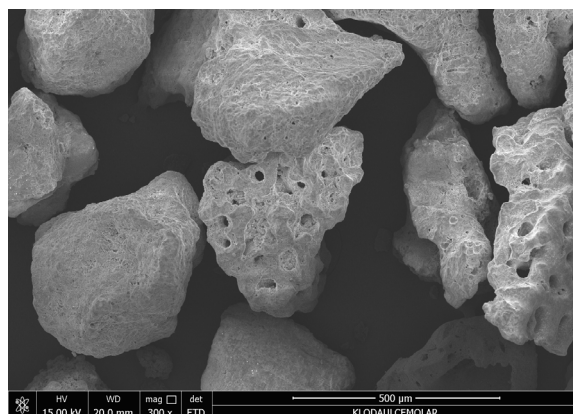


Figure 1. SEM image of calcareous sand.

The $\text{Pb}(\text{NO}_3)_2$, CuSO_4 , and CdCl_2 reagents used in the experiments were analytically pure, and an appropriate amount of the reagents were taken by an analytical balance (CP214, Ohaus Instruments (Shanghai) Co., Ltd., Shanghai, China) and dissolved in a volumetric flask containing 1 L of distilled water to prepare a stock solution with a concentration of 2000 mg/L. The $\text{Pb}(\text{II})$, $\text{Cu}(\text{II})$ and $\text{Cd}(\text{II})$ solutions used in the experiments were diluted from the stock solution.

2.2. Batch Tests

The flasks were numbered and put in a constant-temperature oscillator (SHA-C, Guohua Electric Appliance Co., Ltd., China). Under constant temperature conditions, the speed was controlled at 120 rpm, and the oscillation time was 12 h. This oscillating time was sufficient for the adsorption equilibrium to be reached during the kinetic experiments. During the kinetic tests, the samples were taken at 5 min, 10 min, 15 min, 20 min, 30 min, 40 min, 50 min, 60 min, 90 min, 120 min, then subsequently at 1 h intervals until the solution concentration remained stable. The oscillated solution was passed through a high-speed refrigerated centrifuge (CT15RT, Shanghai Tianmei Biochemical Equipment Engineering Co., Ltd., Shanghai, China) at 5000 rpm for 10 min for solid–liquid separation. The concentration and pH of heavy metal ions in the supernatant were measured by an atomic absorption spectrophotometer (AA60000, Shanghai Tianmei Biochemical Equipment Engineering Co., Ltd., Shanghai, China) and a pH meter (FIVEEASY PLUS 28, Mettler–Toledo Instruments Co. Ltd., Shanghai, China), respectively.

The adsorption (q_e) and removal rate (R) were calculated as follows:

$$q_e = \frac{(C_0 - C_e) \times V}{m} \quad (1)$$

$$R(\%) = \frac{C_0 - C_e}{C_0} \times 100\% \quad (2)$$

where C_0 and C_e are the initial and equilibrium concentrations (mg/L), respectively, of Pb(II), Cu(II) or Cd(II); V is the volume of the solution (L); and m is the mass of calcareous sand (g).

3. Results and Discussion

3.1. Influence of the Solid–Liquid Ratio on the Removal Rate

To analyze the influence of solid–liquid ratio on removal rate, the ratio of solid to liquid r (ratio of adsorbent mass to solution volume) was adjusted between $r = 0.2$ g/L and 2.0 g/L for $C_0 = 1000$ mg/L at 30 °C without pH adjustment, and the influence of the adsorption quantity and removal rate of heavy metal ions were analyzed, as shown in Figure 2.

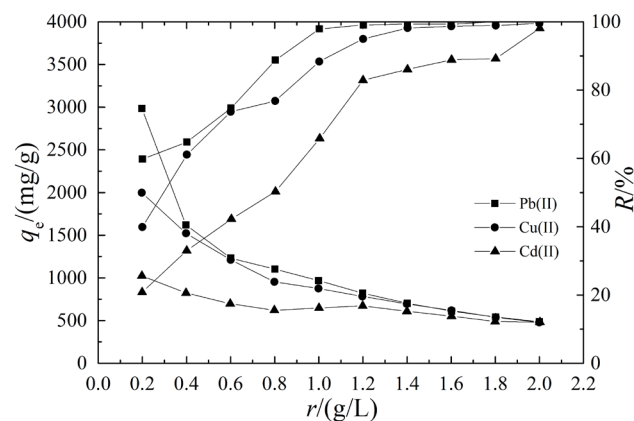


Figure 2. Influence of the solid–liquid ratio on the adsorption of Pb(II), Cu(II) and Cd(II) by calcareous sand.

The experimental results are consistent with the expected results. With increasing solid–liquid ratio, the removal rates by calcareous sand enhance correspondingly, and the adsorption quantity decreases. The reason is that as the amount of calcareous sand is increased, the active adsorption sites exposed to the solution also increase, which is favorable for the complexation and ion exchange of calcium ions with heavy metal ions; therefore, the removal rates increase. When the solid–liquid ratio reaches a certain limit, due to the particle aggregation caused by the increase of calcareous sand content, the active adsorption sites are not fully exposed, the total surface area is reduced, and the diffusion path is increased, resulting in a decrease in adsorption quantity [35]. When $r = 1.0$ g/L, the adsorption quantity of calcareous sand for Pb(II), Cu(II) and Cd(II) can be as high as 975.8 mg/g, 881.54 mg/g and 657.25 mg/g, respectively, with 97.60%, 88.15%, and 65.72% removal rates, respectively. Thus, calcareous sand has a strong adsorption effect on heavy metal ions.

3.2. Influence of the Initial pH_0 on the Removal Rate

To investigate the effect of pH on the adsorption of heavy metal ions by calcareous sand, HNO_3 and $NaOH$ solutions were added to adjust the initial pH_0 under $r = 1.0$ g/L and $C_0 = 1000$ mg/L at 25 °C, and the effect on the removal rate was analyzed.

A study has shown that [36] when the solution $pH > 6$, the contents of Pb^{2+} , Cu^{2+} , Cd^{2+} in the solution are significantly reduced, and the contents of $X(OH)^-$ and $X(OH)_2$ are significantly increased (X is the heavy metal ion). It is found in the experiments that when the $pH > 5$, if no complexing agent is added, the heavy metal ions in the solution begin to precipitate in a small amount. When the $pH < 2$, the solid–liquid interface of the calcareous sand is easily disrupted. For this reason, the pH was controlled in the range of 2 to 5 during our experiments. Figure 3 shows the test results.

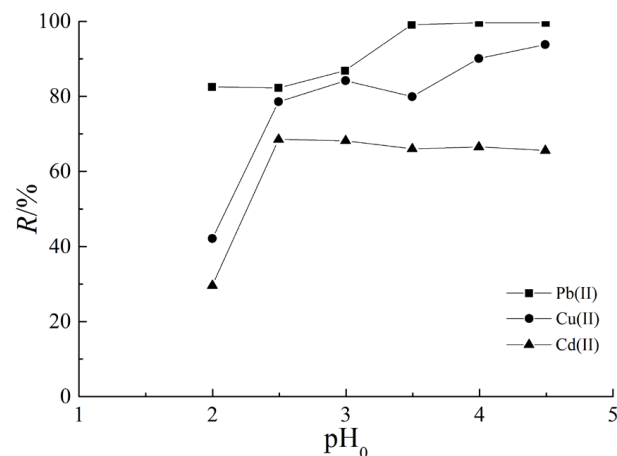


Figure 3. Influence of pH_0 on the adsorption of Pb(II), Cu(II) and Cd(II) by calcareous sand.

The adsorption of heavy metal ions by calcareous sand are all greatly affected by pH_0 . For Pb(II), when $\text{pH} < 3.5$, the removal rate increases with increasing pH_0 . When $\text{pH}_0 > 3.5$, the removal rate essentially reaches the maximum adsorption quantity. For Cu(II), the removal is significantly affected by pH_0 . When $\text{pH} = 2.5$, the removal rate is only 44.9% of the maximum removal rate, and the removal rate is gradually increased with increasing pH. The removal rate of Cd(II) decreases significantly when $\text{pH} < 2.5$. When $\text{pH} > 2.5$, the rate is almost stable with a slight decrease. A comparison of the equilibrium pH_e and pH_0 indicates that the pH_e of the solution increases after the adsorption reaction is completed. When $\text{pH} = 2$, pH_e is stable in the range of 2.68–2.73; when $\text{pH}_0 > 2.5$, the equilibrium pH_e increases to 5.06–5.28. The reasons are analyzed as follows:

- (1) In the solution with lower pH, the H^+ content is high. H^+ has a stronger adsorption point binding ability than heavy metal ions. H^+ competes and occupies more adsorption sites. At the same time, some calcium sand is dissolved by acid at low pH, resulting in a decrease in the removal rate.
- (2) Due to the difference in the attractive force of the active sites such as $-\text{CO}_3^{2-}$ and $-\text{Ca}^{2+}$, $-\text{Mg}^{2+}$, for H^+ or OH^- in aqueous solution, a certain charge exists. When the pH of the solution is low, due to protonation, there is a large amount of H^+ resulting in a positive charge. A strong repulsion exists between Pb^{2+} , which is not favorable for adsorption; as the pH increases, the surface of the calcareous sand deprotonates, the proton concentration decreases, and the positive charge on the surface is reduced, which reduces the competitive adsorption of H^+ and surface complexes on metal ions. These conditions are favorable for adsorption and tend to increase the adsorption quantity [4,37].
- (3) The slight increase in pH after the reaction is caused by the surface complexation reaction and the consumption of H^+ by the calcium components [5].

The pH of industrial wastewater is in the range of 4–7. Therefore, calcareous sand has a certain practical significance as an adsorbent in practical operation.

3.3. Influence of Ionic Strength on the Removal Rate

To explore the influence of ionic strength on the adsorption of calcareous sand, the ionic strength of NaCl was adjusted in the range of 0–0.6 mol/L to analyze its effect on the adsorption of Pb(II) by calcareous sand under the conditions of $r = 1.0$ g/L and $C_0 = 1000$ mg/L without adjusting the pH. The experimental results are shown in Figure 4.

Overall, with increasing Na^+ ionic strength, the removal rate of Pb(II) by calcareous sand decreases, and its adsorption ability decreases, indicating that competition exists between Na^+ and Pb^{2+} [38]. The addition of NaCl solution causes the counter ions to surround the oppositely charged adsorption sites and partially neutralize the adsorption site charge [39], thereby inhibiting adsorption. The adsorption mechanisms of calcium

sand include electrostatic interaction, complexation reaction and ion exchange, among other effects [40,41]. When the Na^+ ionic strength is less than a certain value, its existence compresses the thickness of the electron double layer of calcareous sand, the thickness of the diffusion layer is reduced by compression, the collision distance between Pb^{2+} and calcareous sand decreases, and the adsorption quantity increases slightly. When the Na^+ ionic strength continues to increase, Na^+ competes with Pb^{2+} for adsorption sites, resulting in a slight decrease in Pb^{2+} adsorption. Considering that there may be chemical bonds between Pb^{2+} and calcareous sand, inner-sphere surface complexes (ISSC) can be formed [42–44].

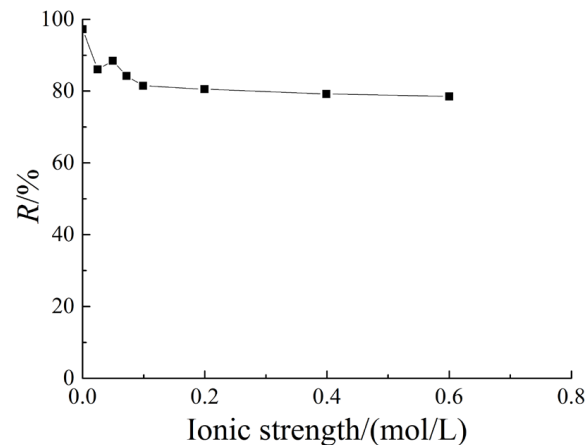


Figure 4. Influence of ionic strength on the removal of Pb(II) by calcareous sand.

Understanding the adsorption mechanism was conducive to interdisciplinary development [45–47]. The hydrated ionic radius of Pb^{2+} is 0.401 nm. From the ionic radius point of view, it is easier to complex with the $-\text{CO}_3^{2-}$ adsorption sites, so the surface-complexing adsorption dominates in the adsorption mechanism [48,49], together with ion exchange reactions. The PbCO_3 precipitation could be observed by scanning electron microscopy on the adsorbent surface at a low Pb(II) concentration, indicating that the adsorption process is accompanied by a surface precipitation phenomenon [50].

3.4. Adsorption Kinetics Characteristics

At $T = 30\text{ }^\circ\text{C}$, $r = 1.0\text{ g/L}$, and $C_0 = 1000$ (Pb(II)), 1250 (Cu(II)), and 1500 (Cd(II)) mg/L, the adsorption reaction process of calcareous sand was studied. Figure 5 shows the experimental results.

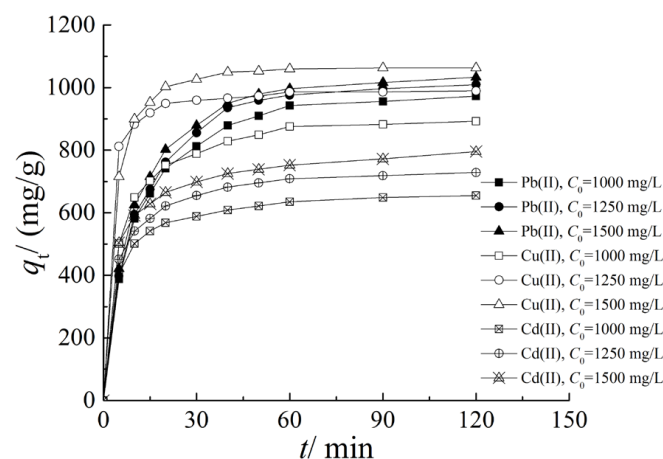


Figure 5. Influence of reaction time on the adsorption of Pb(II), Cu(II) and Cd(II) by calcareous sand.

The adsorption process of calcium sand for Pb(II), Cu(II) and Cd(II) is a rapid reaction: the removal rate can reach 80% of the maximum removal rate at 30 min, and the equilibrium state can be reached within 120 min. In the initial reaction stage, the adsorption sites are abundant; Pb(II), Cu(II) and Cd(II) have large concentration differences at the solid–liquid interface [51], and the adsorption reaction is quick. As the reaction progresses, the reaction rate decreases because the adsorption site is reduced. The concentration of heavy metal ions also decreases. The concentration difference between the solution and the adsorbent is decreased. The average collision distance of the remaining Pb(II), Cu(II), and Cd(II) is increased, and the diffusion rate inside the particles slows down.

To analyze the adsorption kinetics of calcareous sand for heavy metal ions, the pseudo-second-order kinetic model was used to analyze the kinetic experimental data.

The pseudo-second-order dynamic equation can be expressed as [52]

$$\frac{dq_t}{dt} = k_2(q_e - q_t)^2 \quad (3)$$

Its integral can be converted into a linear form

$$\frac{t}{q_t} = \frac{1}{k_2 q_e^2} + \frac{t}{q_e} \quad (4)$$

where k_2 is the pseudo-second-order kinetic adsorption rate constant ($\text{g} \cdot \text{mg}^{-1} \cdot \text{min}^{-1}$).

The initial adsorption rate can be expressed as

$$h = k_2 q_e^2 \quad (5)$$

The pseudo-second-order kinetic model is applied to fit the experiment results. The fitting parameters and fitting curve are shown in Table 1 and Figure 6, respectively.

The determination coefficients are high, and the calculated equilibrium adsorption quantity is close to the measured values at 120 min, indicating that the pseudo-second-order kinetic model can well characterize the adsorption kinetics of calcareous sand. Cu(II) has the highest adsorption rate, and Cd(II) has the lowest adsorption quantity.

Table 1. Pseudo-second-order kinetic model parameters of Pb(II), Cu(II) and Cd(II) adsorption by calcareous sand.

Ion	Parameters	$C_0/(\text{mg/L})$		
		1000	1250	1500
Pb(II)	$q_{e,\text{exp}}/(\text{mg/g})$	973.8	1014.1	1022.9
	$q_{e,\text{cal}}/(\text{mg/g})$	1043.2	1088.9	1103.6
	$h/(\text{mg/g/min})$	134.0	137.9	150.9
	$k_2 \times 10^{-4}/(\text{g/mg/min})$	1.231	1.163	1.239
	R^2	0.9996	0.9992	0.9996
Cu(II)	$q_{e,\text{exp}}/(\text{mg/g})$	894.56	986.63	1065.35
	$q_{e,\text{cal}}/(\text{mg/g})$	927.72	997.50	1085.74
	$h/(\text{mg/g/min})$	215.81	947.81	577.64
	$k_2 \times 10^{-4}/(\text{g/mg/min})$	2.50	9.52	4.90
	R^2	0.9999	0.9999	0.9998
Cd(II)	$q_{e,\text{exp}}/(\text{mg/g})$	657.3	729.71	795.53
	$q_{e,\text{cal}}/(\text{mg/g})$	676.72	752.38	818.18
	$h/(\text{mg/g/min})$	184.18	198.65	194.59
	$k_2 \times 10^{-4}/(\text{g/mg/min})$	4.021	3.50	2.90
	R^2	0.9999	0.9999	0.9995

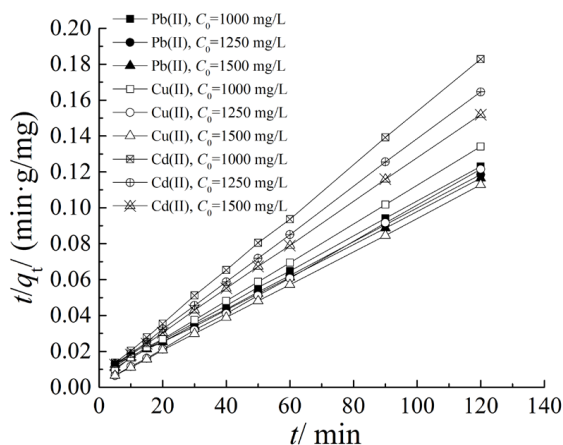


Figure 6. Fitting curves obtained from the pseudo-second-order dynamics model.

3.5. Isothermal Adsorption Characteristics

At $r = 1.0 \text{ g/L}$, temperatures of $30 \text{ }^\circ\text{C}$, $40 \text{ }^\circ\text{C}$, and $50 \text{ }^\circ\text{C}$ and a reaction time of 12 h, with a changing initial concentration of heavy metal ions (1000–2000 mg/L), the isothermal adsorption characteristics of calcareous sand were studied. The test results are shown in Figure 7.

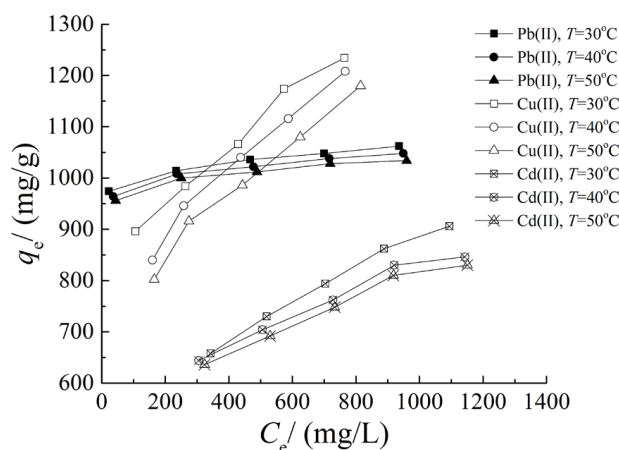


Figure 7. Isothermal adsorption characteristic curves of Pb(II), Cu(II) and Cd(II) by calcareous sand at different temperatures.

The equilibrium adsorption of heavy metal ions by calcareous sand exhibit an increasing trend with increasing initial concentration. This result arises because the adsorption reaction occurs mainly on the calcareous sand surface in full contact with the aqueous solution when the Pb(II), Cu(II) and Cd(II) initial concentrations are low. Nevertheless, with the increasing initial concentration, the heavy metal ions continue to diffuse into the calcareous sand, and the driving force of the adsorption reaction increases, so the adsorption quantity also increases. Moreover, the adsorption quantity decreases as the temperature increases; therefore, the adsorption of heavy metal ions onto calcareous sand is an exothermic process, for which a temperature rise is unfavorable. The isothermal adsorption lines are convex type I curves, suggesting that attraction exists between the calcareous sand and the heavy metal ions to promote adsorption [53].

To investigate the adsorption process of calcareous sand, the Langmuir model was employed to fit the experimental data.

The Langmuir model can be expressed as

$$\frac{C_e}{q_e} = \frac{1}{bQ_m} + \frac{C_e}{Q_m} \tag{6}$$

where Q_m is the maximum single-layer saturated adsorption quantity (mg/g) and b is the Langmuir constant (L/mg), which is related to the adsorption free energy.

Following linear fitting of the experimental results, the fitting curve is shown in Figure 8, and Table 2 shows the model parameters. This model shows a good fit with the isothermal adsorption process, which indicates that a certain concentration of Pb(II), Cu(II), Cd(II) forms complex structures with calcareous sand through co-ordination bonds and that monomolecular adsorption occurs.

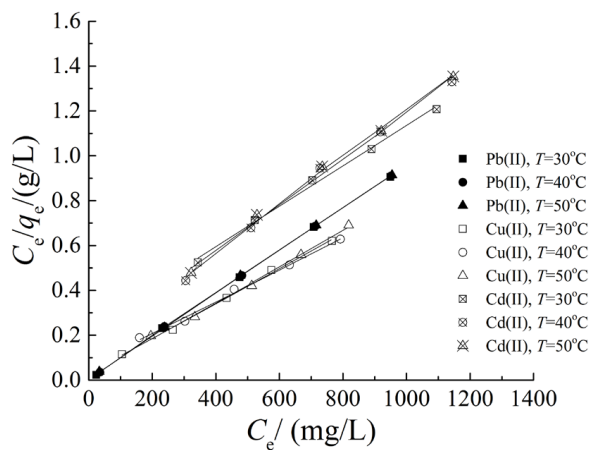


Figure 8. Fitting curve of the Langmuir model.

Table 2. Langmuir model parameters of Pb(II), Cu(II) and Cd(II) adsorption by calcareous sand.

Ion	Parameters	Temperature/(°C)		
		30	40	50
Pb(II)	Q_m /(mg/g)	1052.95	1052.74	1050.41
	b /(L/mg)	0.315	0.116	0.421
	$R_L \times 10^{-3}$	3.679	4.257	1.186
	R^2	0.999	0.999	0.999
Cu(II)	Q_m /(mg/g)	1329.84	1289.01	1247.07
	b /(L/mg)	0.013	0.013	0.032
	$R_L \times 10^{-3}$	0.037	0.036	0.015
	R^2	0.997	0.995	0.995
Cd(II)	Q_m /(mg/g)	1050.56	892.59	841.93
	b /(L/mg)	0.004	0.016	0.009
	$R_L \times 10^{-3}$	0.114	0.030	0.054
	R^2	0.997	0.992	0.994

The expression of the dimensionless separation factor R_L , which reflects the ease of adsorption defined by the Langmuir model, is

$$R_L = \frac{1}{1 + bC_0} \tag{7}$$

where C_0 is the highest concentration value of the initial adsorbate. We have $R_L < 1$ for the isothermal adsorption results of calcium sand for heavy metal ions, indicating that it is favorable for the adsorption reactions, which are all preferential adsorption processes [54].

The adsorption by calcareous sand is influenced by the adsorption sites and the metal ions themselves. The adsorption mechanisms of calcareous sand include electrostatic interaction, complexation reaction and ion exchange, among other mechanisms [40,41]. Thermodynamic calculations reveal that the adsorption of metal ions by calcareous sand is dominated by physical adsorption. When the adsorption is dominated by electrostatic interaction, the adsorption performance of the adsorbent is greatly affected by the electronegativity and the hydrated ionic radius of the metal ions. Typically, a smaller ionic radius makes it easier to bond with the adsorption sites. Meanwhile, the greater the electronegativity of the metal ion itself, the stronger the electrostatic interaction.

The electronegativity order of the three metals is Cu (1.9), Pb (1.85), and Cd (1.52). Their hydrated ionic radii are Pb (0.401 nm), Cu (0.419 nm), and Cd (0.426 nm) [55]. In addition, Pb(II), Cu(II) and Cd(II) have different reaction modes and adsorption products on the adsorbent surface. The reaction modes of Cu(II) and Cd(II) are dominated by ion exchange and surface co-ordination, and the products exist in multi- and mono-core binding states. Pb(II) is dominated by surface precipitation and co-ordination adsorption, and its product is in precipitation form [50]. As a result of combined effects, the adsorption ability of calcareous sand for heavy metal ions follows the electronegativity order. Although the hydrated ionic radius of Cu^{2+} is larger than that of Pb^{2+} , the affinities of calcareous sand to the three metal ions are $\text{Cu} > \text{Pb} > \text{Cd}$.

3.6. Adsorption Thermodynamic Characteristics

To analyze the influence of temperature on adsorption process, they were studied through experiments at different temperatures. By calculating the thermodynamic parameters and analyzing the change in the adsorption free energy, the adsorption mechanism is further deduced. The free energy change for physical adsorption is -20 to 0 kJ/mol, and the free energy change for chemical adsorption is -400 to 80 kJ/mol.

(1). The enthalpy change ΔH can be expressed as

$$\ln \frac{1}{C_e} = \ln K_0 + \left(-\frac{\Delta H}{RT} \right) \quad (8)$$

where T is the temperature (K), ΔH is the enthalpy change ($\text{kJ} \cdot \text{mol}^{-1} \cdot \text{T}^{-1}$), and K_0 is the constant of the Van't Hoff equation.

(2). The free energy change ΔG is calculated by

$$\Delta G = -RT \ln K_d \quad (9)$$

where ΔG is the free energy change (kJ/mol), R is the gas molar constant ($8.314 \text{ kJ} \cdot \text{mol}^{-1} \cdot \text{T}^{-1}$), and K_d is the adsorption thermodynamic equilibrium constant ($K_d = q_e/C_e$) [56–60].

(3). The entropy change ΔS is calculated by

$$\Delta S = \frac{\Delta H - \Delta G}{T} \quad (10)$$

According to the experimental data of isothermal adsorption of calcareous sand at different initial concentrations and temperatures, the fitting curve can be obtained by fitting through Formula (8) and calculating through Formula (9) and (10) (Figure 9). Table 3 lists the related parameters.

The results show that the adsorption enthalpy change $\Delta H < 0$, revealing that the adsorption reaction is an exothermic reaction, which is unfavorable for adsorption behavior of calcareous sand when temperature rises. For Pb(II) and Cu(II), $\Delta G < 0$, the reaction can proceed spontaneously. At the same time, $\Delta G < 0$ is all within the range of -20 to 0 kJ/mol, revealing that the adsorption of Pb(II) and Cu(II) by calcareous sand is mainly physical adsorption. For Cd(II), when $C_0 < 1500$ mg/L, $\Delta G < 0$, and the adsorption behavior proceeds spontaneously, mainly by physical adsorption; when $C_0 > 1500$ mg/L, $\Delta G > 0$,

indicating that the reaction is driven mainly by the concentration difference within the solid–liquid interface.

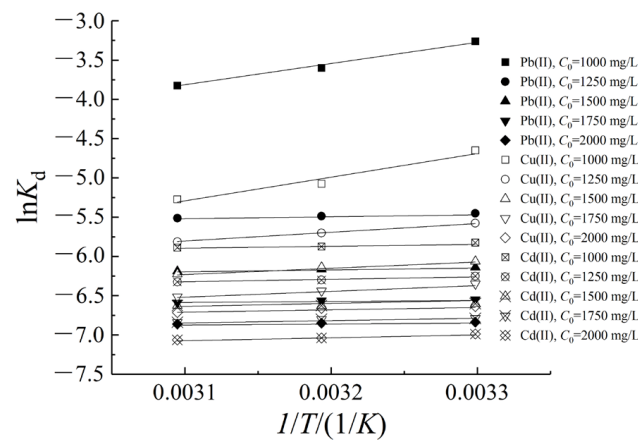


Figure 9. Van't Hoff formula linear fitting for the adsorption of Pb(II), Cu(II) and Cd(II) by calcareous sand.

Table 3. Thermodynamic parameters of the adsorption of Pb(II), Cu(II) and Cd(II) by calcareous sand.

Ion	Parameters	T/(K)	C ₀ /(mg/L)				
			1000	1250	1500	1750	2000
Pb(II)	ΔG/(kJ/mol)	303.15	−9.12	−3.68	−2	−1.01	−0.32
		313.15	−8.51	−3.71	−1.99	−0.97	−0.26
		323.15	−8.17	−3.71	−1.97	−0.96	−0.18
	ΔS × 10 ^{−2} /(J/mol/K)	303.15	−4.5	0.38	0.1	−0.03	−0.25
		313.15	−4.55	0.38	0.09	−0.05	−0.27
		323.15	−4.52	0.36	0.08	−0.05	−0.29
	ΔH/(kJ/mol)	-	−22.76	−2.54	−1.7	−1.12	−1.09
R ²	-	0.999	0.999	0.999	0.979	0.997	
Cu(II)	ΔG/(kJ/mol)	303.15	−5.39	−3.33	−2.26	−1.8	−1.2
		313.15	−4.3	−2.96	−2.13	−1.48	−1.1
		323.15	−3.78	−2.7	−1.75	−1.29	−0.99
	ΔS × 10 ^{−2} /(J/mol/K)	303.15	−0.07	−0.02	−0.02	−0.01	0.01
		313.15	0.01	0.01	0.01	0.01	0.01
		323.15	0.01	0.01	0.01	0.01	0.01
	ΔH/(kJ/mol)	-	−25.44	−9.77	−6.81	−6.11	−2.7
R ²	-	0.983	0.996	0.976	0.992	0.999	
Cd(II)	ΔG/(kJ/mol)	303.15	−1.64	−0.85	−0.31	0.08	0.47
		313.15	−1.54	−0.66	−0.09	0.26	0.8
		323.15	−1.5	−0.57	−0.02	0.4	0.92
	ΔS × 10 ^{−2} /(J/mol/K)	303.15	−0.003	−0.007	−0.008	−0.008	−0.011
		313.15	0.005	0.002	0.001	−0.001	−0.003
		323.15	0.005	0.002	0.001	−0.001	−0.003
	ΔH/(kJ/mol)	-	−2.47	−2.91	−2.68	−2.29	−2.72
R ²	-	0.988	0.984	0.98	0.993	0.956	

4. Conclusions

The adsorption characteristics of calcareous sand for heavy metal ions have been studied by batch testing, and the influence of pH, ionic strength, temperature and reaction time has been explored. Through the comprehensive analysis of a large amount of experimental data, the following conclusions are obtained.

- (1) The initial pH and the solid–liquid ratio have a significant influence on the removal efficiency. At $T = 30\text{ }^{\circ}\text{C}$, $r = 1.0\text{ g/L}$, and $C_0 = 1000\text{ mg/L}$ and for 12 h of reaction time, the removal efficiencies of Pb(II), Cu(II) and Cd(II) are 97.6%, 88.15% and 65.72%, respectively.

- (2) The optimal adsorption pH of calcareous sand is between 3.5 and 5.0. Strong acids and higher temperatures are not favorable for the adsorption by calcareous sand. As the ionic strength increases, the adsorption ability of calcareous sand decreases.
- (3) At 60 min, the adsorption quantity reaches 80% of the maximum adsorption quantity, and the equilibrium can be reached within 120 min. The pseudo-second-order kinetic model is suitable to simulate the dynamic adsorption process of calcareous sand, and the isothermal process is found to obey the Langmuir model.
- (4) Thermodynamic test results indicate that the adsorption process is spontaneously exothermic and that low temperature is favorable to the adsorption reaction.
- (5) Calcareous sand has a very high adsorption capacity for Pb(II), Cu(II) and Cd(II), with a maximum adsorption quantity Q_m of 1052.95 mg/g, 1329.84 mg/g and 1050.56 mg/g, respectively, indicating that calcareous sand can be used as a potential adsorbent for wastewater treatment.

Author Contributions: Conceptualization, J.Z. and G.L.; methodology, J.Z. and G.L.; validation, J.L. and D.Y.; writing—original draft preparation, G.L.; writing—review and editing, J.Z.; funding acquisition, G.L. All authors have read and agreed to the published version of the manuscript.

Funding: This research was funded by Natural Science Basic Research Program of Shaanxi Province, grant number 2021JM-535 and Special Fund for Scientific Research by Xijing University, grant number XJ18T01.

Data Availability Statement: Not applicable.

Conflicts of Interest: The authors declare no conflict of interest.

References

1. Xiao, C.K. Analysis of present situation about lead pollution in China. *Environ. Sustain. Dev.* **2017**, *42*, 91–92.
2. Lin, B.L.; Wu, L.L.; Cui, S.; Shen, X.D.; Zhang, X.Z.; Zhou, Y. Research progress of novel adsorbents of heavy metal ions. *Mater. Rev.* **2015**, *29*, 18–23.
3. Fu, F.; Wang, Q. Removal of heavy metal ions from wastewaters: A review. *J. Environ. Manag.* **2011**, *92*, 407–418. [[CrossRef](#)] [[PubMed](#)]
4. Zhang, J.L.; Zhang, L.L. Adsorption behaviors of heavy metal Pb(II) on clay. *Chin. J. Geotech. Eng.* **2012**, *34*, 1584–1589.
5. Zhang, J.L.; Liu, D.W.; Yang, Q. Adsorption behaviors of bone char to heavy metal Pb(II). *Chin. J. Environ. Eng.* **2014**, *8*, 1784–1790.
6. Zhang, J.L.; Li, Y. Adsorption behaviors of lead on multi-walled carbon nanotube-hydroxyapatite composites. *Environ. Sci.* **2015**, *36*, 2554–2563.
7. Shi, Y.T.; Zhang, J.L.; Yang, Q. Adsorption behaviors of Pb(II) on white pottery clay. *J. Dalian Univ. Technol.* **2016**, *56*, 396–405.
8. Li, Z.Z.; Tang, X.W.; Chen, Y.M.; Wang, Y. Sorption behavior and mechanism of Pb(II) on Chinese loess. *J. Environ. Eng.* **2009**, *135*, 58–67. [[CrossRef](#)]
9. Saha, P.; Datta, S.; Sanyal, S.K. Application of natural clayey soil as adsorbent for the removal of copper from wastewater. *J. Environ. Eng.* **2010**, *136*, 1409–1417. [[CrossRef](#)]
10. Abdel-Halim, S.H.; Shehata, A.M.A.; El-Shahat, M.F. Removal of lead ions from industrial waste water by different types of natural materials. *Water Res.* **2003**, *37*, 1678–1683. [[CrossRef](#)]
11. Singh, S.P.; Ma, L.Q.; Hendry, M.J. Characterization of aqueous lead removal by phosphatic clay: Equilibrium and kinetic studies. *J. Hazard. Mater.* **2006**, *136*, 654–662. [[CrossRef](#)] [[PubMed](#)]
12. Vieira, M.G.A.; Neto, A.F.A.; Gimenes, M.L.; Silva, M.G.C. Sorption kinetics and equilibrium for the removal of nickel ions from aqueous phase on calcined Bofe bentonite clay. *J. Hazard. Mater.* **2010**, *177*, 362–371. [[CrossRef](#)]
13. Priyantha, N.; Bandaranayaka, A. Investigation of kinetics of Cr(VI)-fired brick clay interaction. *J. Hazard. Mater.* **2011**, *188*, 193–197. [[CrossRef](#)] [[PubMed](#)]
14. Djukić, A.; Jovanović, U.; Tuvčić, T.; Andrić, V.; Novaković, J.G.; Ivanović, N.; Matovića, L. The potential of ball-milled Serbian natural clay for removal of heavy metal contaminants from wastewaters: Simultaneous sorption of Ni, Cr, Cd and Pb ions. *Ceram. Int.* **2013**, *39*, 7173–7178. [[CrossRef](#)]
15. Du, Y.J.; Hayashi, S. A study on sorption properties of Cd²⁺ on Ariake clay for evaluating its potential use as a landfill barrier material. *Appl. Clay Sci.* **2006**, *32*, 14–24. [[CrossRef](#)]
16. Mouni, L.; Merabet, D.; Robert, D.; Bouzaza, A. Batch studies for the investigation of the sorption of the heavy metals Pb²⁺ and Zn²⁺ onto Amizour soil (Algeria). *Geoderma* **2009**, *154*, 30–35. [[CrossRef](#)]
17. Waseem, M.; Mustafa, S.; Naeem, A.; Shah, K.H.; Shah, I. Mechanism of Cd (II) sorption on silica synthesized by sol-gel method. *Chem. Eng. J.* **2011**, *169*, 78–83. [[CrossRef](#)]

18. Putz, A.M.; Ivankov, O.I.; Kuklin, A.I.; Ryukhtin, V.; Ianasi, C.; Ciopec, M.; Negrea, A.; Trif, L.; Horvath, Z.E.; Almasly, L. Ordered mesoporous silica prepared in different solvent conditions: Application for Cu(II) and Pb(II) adsorption. *Gels* **2022**, *8*, 443. [[CrossRef](#)]
19. Habte, L.; Shiferaw, N.; Khan, M.D.; Thriveni, T.; Ahn, J.W. Sorption of Cd²⁺ and Pb²⁺ on aragonite synthesized from eggshell. *Sustainability* **2020**, *12*, 1174. [[CrossRef](#)]
20. Vu, T.N.; Le, P.H.P.; Pham, D.N.P.; Hoang, T.H.; Nadda, A.K.; Le, T.S.; Pham, T.D. Highly adsorptive protein inorganic nanohybrid of Moringa seeds protein and rice husk nanosilica for effective adsorption of pharmaceutical contaminants. *Chemosphere* **2022**, *307*, 135856. [[CrossRef](#)]
21. Truong, T.T.; Le, T.H.; Pham, T.D. Adsorption characteristics of Copper (II) ion on Cu-doped ZnO nanomaterials based on green synthesis from *Piper chaudiocann*, L. leaves extract. *Colloid Polym. Sci.* **2022**, *300*, 1343–1354. [[CrossRef](#)]
22. Selmy, S.A.H. Inorganic and organic ligands induced changes in Pb sorption of arid clay and calcareous loamy sand soils. *Arch. Agron. Soil Sci.* **2018**, *64*, 1582–1594. [[CrossRef](#)]
23. Elbana, T.A.; Selim, H.M. Lead mobility in calcareous soils: Influence of cadmium and copper. *Soil Sci.* **2013**, *178*, 417–424. [[CrossRef](#)]
24. Lv, B.F.; Yu, W.J.; Luo, J.L.; Qian, B.; Asefa, M.B.; Li, N. Study on the adsorption mechanism of graphene oxide by calcareous sand in South China Sea. *Adsorpt. Sci. Technol.* **2021**, *2021*, 2227570. [[CrossRef](#)]
25. Salzman, S.A.; Allinson, G.; Stagnitti, F.; Hill, R.J.; Thwaites, L.; Ierodiaconou, D.; Carr, R.; Sherwood, J.; Versace, V. Adsorption and desorption characteristics of fluoride in the calcareous and siliceous sand sheet aquifers of south-west Victoria, Australia. *WIT Trans. Ecol. Environ.* **2008**, *111*, 159–174.
26. Ranjbar, F.; Jalali, M. Measuring and modeling ammonium adsorption by calcareous soils. *Environ. Monit. Assess.* **2013**, *185*, 3191–3199. [[CrossRef](#)] [[PubMed](#)]
27. Baghenejad, M.; Javaheri, F.; Moosavi, A.A. Adsorption isotherms of some heavy metals under conditions of their competitive adsorption onto highly calcareous soils of southern Iran. *Arch. Agron. Soil Sci.* **2016**, *62*, 1462–1473. [[CrossRef](#)]
28. Ghiri, M.N.; Rezaei, M.; Sameni, A. Zinc sorption-desorption by sand, silt and clay fractions in calcareous soils of Iran. *Arch. Agron. Soil Sci.* **2012**, *58*, 945–957. [[CrossRef](#)]
29. Moharami, S.; Jalali, M. Effects of cations and anions on iron and manganese sorption and desorption capacity in calcareous soils from Iran. *Environ. Earth Sci.* **2013**, *68*, 847–858. [[CrossRef](#)]
30. Mashal, K.; Al-Degs, Y.S.; Al-Qinna, M.; Salahat, M. Elucidation of phosphorous sorption by calcareous soils using principal component analysis. *Chem. Ecol.* **2014**, *30*, 133–146. [[CrossRef](#)]
31. Ouachtak, H.; Akhouairi, S.; Addi, A.A.; Akbour, R.A.; Jada, A.; Douch, J.; Hamdani, M. Mobility and retention of phenolic acids through a goethite-coated quartz sand column. *Colloids Surf. A* **2018**, *546*, 9–19. [[CrossRef](#)]
32. Ouachtak, H.; Akhouairi, S.; Haounati, R.; Addi, A.A.; Jada, A.; Taha, M.L.; Douch, J. 3, 4-Dihydroxybenzoic acid removal from water by goethite modified natural sand column fixed-bed: Experimental study and mathematical modeling. *Desalin. Water Treat.* **2020**, *194*, 439–449. [[CrossRef](#)]
33. Chen, H.Y. *Study on the Inner Pore in Calcareous Sand*; Graduate School of the Chinese Academy of Sciences, Wuhan Institute of Rock and Soil Mechanics: Wuhan, China, 2005.
34. Lv, B.L. Engineering parameters of calcareous coral sand. *Constr. Technol.* **2015**, *44*, 146–148.
35. Balasubramanian, R.; Perumal, S.V.; Vijayaraghavan, K. Equilibrium isotherm studies for the multicomponent adsorption of Lead, Zinc, and Cadmium onto Indonesian peat. *Ind. Eng. Chem. Res.* **2009**, *48*, 2093–2099. [[CrossRef](#)]
36. Montazer-Rahmati, M.M.; Rabbani, P.; Abdolali, A.; Keshkar, A.R. Kinetics and equilibrium studies on biosorption of cadmium, lead, and nickel ions from aqueous solutions by intact and chemically modified brown algae. *J. Hazard. Mater.* **2011**, *185*, 401–407. [[CrossRef](#)] [[PubMed](#)]
37. Yuan, Y.H.; Lei, L.; He, H.; Jia, D.M. Study on the adsorption of copper ions by epichlorohydrin-crosslinked chitosan/sodium alginate adsorbent. *J. South China Univ. Technol. Nat. Sci.* **2012**, *40*, 148–154.
38. Lützenkirchen, J. Ionic strength effects on cation sorption to oxides: Macroscopic observations and their significance in microscopic interpretation. *J. Colloid Interface Sci.* **1997**, *195*, 149–155. [[CrossRef](#)]
39. Vilar, V.J.P.; Botelho, C.M.S.; Boaventura, R.A.R. Influence of pH, ionic strength and temperature on lead biosorption by Gelidium and agar extraction algal waste. *Process Biochem.* **2005**, *40*, 3267–3275. [[CrossRef](#)]
40. Liu, H.N.; Qing, B.J.; Ye, X.S.; Li, Q.; Lee, K.; Wu, Z.J. Boron adsorption by composite magnetic particles. *Chem. Eng. J.* **2009**, *151*, 235–240. [[CrossRef](#)]
41. Wu, Z.J.; You, L.J.; Xiang, H.; Jiang, Y. Comparison of dye adsorption by mesoporous hybrid gels: Understanding the interactions between dyes and gel surfaces. *J. Colloid Interface Sci.* **2006**, *303*, 346–352. [[CrossRef](#)]
42. Goldberg, S. Inconsistency in the triple layer model description of ionic strength dependent boron adsorption. *J. Colloid Interface Sci.* **2005**, *285*, 509–517. [[CrossRef](#)]
43. Wu, Z.J.; Liu, H.N.; Zhang, H.F. Research progress on mechanisms about the effect of ionic strength on adsorption. *Environ. Chem.* **2010**, *29*, 997–1003.
44. Chen, C.; Wang, X. Sorption of Th(IV) to silica as a function of pH, humic/fulvic acid, ionic strength, electrolyte type. *Appl. Radiat. Isot.* **2007**, *65*, 155–163. [[CrossRef](#)] [[PubMed](#)]

45. Yang, Y.R.; Kulandaivel, A.; Mehrez, S.; Mahariq, I.; Elbadawy, I.; Mohanavel, V.; Jalil, A.T.; Saleh, M.M. Developing a high-performance electromagnetic microwave absorber using BaTiO₃/CoS₂/CNTs triphase hybrid. *Ceram. Int.* **2023**, *49*, 2557–2569. [[CrossRef](#)]
46. Yang, Y.R.; Li, G.; Luo, T.; Al-Bahrani, M.; Al-Ammar, E.A.; Sillanpaa, M.; Ali, S.; Leng, X.J. The innovative optimization techniques for forecasting the energy consumption of buildings using the shuffled frog leaping algorithm and different neural networks. *Energy* **2023**, *268*, 126548. [[CrossRef](#)]
47. Yang, Y.R.; Logesh, K.; Mehrez, S.; Huynen, I.; Elbadawy, I.; Mohanavel, V.; Alamri, S. Rational construction of wideband electromagnetic wave absorber using hybrid FeWO₄-based nanocomposite structures and tested by the free-space method. *Ceram. Int.* **2023**, *49*, 2130–2139. [[CrossRef](#)]
48. Lin, F.F.; Yi, X.Y.; Dang, Z.; Zheng, L.C. Adsorption of Cd²⁺ and Pb²⁺ from aqueous solution by modified peanut shells. *J. Agro Environ. Sci.* **2011**, *30*, 1404–1408.
49. Li, B.; Li, H.; Zhu, H.L.; Tian, R.; Gao, X.D. Dynamic light scattering of aggregation of colloids in yellow earth different in pH. *Acta Pedol. Sin.* **2013**, *50*, 89–95.
50. Wu, H.H.; Wu, D.Q.; Peng, J.L. Experimental study on the surface reactions of heavy metal ion with calcite. *Acta Petrol. Mineral.* **1999**, *18*, 301–308.
51. Ni, H.; Li, Y.L.; Cui, R.P.; Lu, Y.; Yang, G.D. Kinetics and thermodynamics of Cu²⁺ and Pb²⁺ adsorption from aqueous solutions onto dolomite adsorbent. *Chin. J. Environ. Eng.* **2016**, *10*, 3077–3083.
52. Ho, Y.S.; McKay, G. Pseudo-second order model for sorption processes. *Process Biochem.* **1999**, *34*, 451–465. [[CrossRef](#)]
53. Seiichi, K.; Tatsuo, I.; Abe, Y. *Adsorption Science*, 2nd ed.; Chemical Industry Press: Beijing, China, 2006.
54. Conte, L.O.; Schenone, A.V.; Alfano, O.M. Photo-Fenton degradation of the herbicide 2, 4-D in aqueous medium at pH conditions close to neutrality. *J. Environ. Manag.* **2016**, *170*, 60–69. [[CrossRef](#)] [[PubMed](#)]
55. Lazarević, S.; Janković-Castvan, I.; Tanasković, D.; Pavićević, V. Sorption of Pb²⁺, Cd²⁺, and Sr²⁺ ions on calcium hydroxyapatite powder obtained by the hydrothermal method. *J. Environ. Eng.* **2008**, *134*, 683–688. [[CrossRef](#)]
56. Hu, Q.H.; Meng, Y.Y.; Sun, T.X.; Mahmood, Q.; Wu, D.L.; Zhu, J.H.; Lu, G. Kinetics and equilibrium adsorption studies of dimethylamine (DMA) onto ion-exchange resin. *J. Hazard. Mater.* **2011**, *185*, 677–681. [[CrossRef](#)] [[PubMed](#)]
57. Kuang, S.P.; Wang, Z.Z.; Liu, J.; Wu, Z.C. Preparation of triethylene-tetramine grafted magnetic chitosan for adsorption of Pb(II) ion from aqueous solutions. *J. Hazard. Mater.* **2013**, *260*, 210–219. [[CrossRef](#)]
58. Wibowo, E.; Rokhmat, M.; Khairurrijal, S.; Abdullah, M. Reduction of seawater salinity by natural zeolite (Clinoptilolite): Adsorption isotherms, thermodynamics and kinetics. *Desalination* **2017**, *409*, 146–156. [[CrossRef](#)]
59. Rodrigues, L.A.; da Silva, M.L.C.P. Thermodynamic and kinetic investigations of phosphate adsorption onto hydrous niobium oxide prepared by homogeneous solution method. *Desalination* **2010**, *263*, 29–35. [[CrossRef](#)]
60. Zhou, F.; Zhang, Y.X.; Liu, Q.; Huang, S.H.; Wu, X.Y.; Wang, Z.W.; Zhang, L.S.; Chi, R. Modified tailings of weathered crust elution-deposited rare earth ores as adsorbents for recovery of rare earth ions from solutions: Kinetics and thermodynamics studies. *Miner. Eng.* **2023**, *191*, 107937. [[CrossRef](#)]

Disclaimer/Publisher's Note: The statements, opinions and data contained in all publications are solely those of the individual author(s) and contributor(s) and not of MDPI and/or the editor(s). MDPI and/or the editor(s) disclaim responsibility for any injury to people or property resulting from any ideas, methods, instructions or products referred to in the content.